Prediction of Curved Channel Flow with an Extended k-ϵ Model of Turbulence

Farzad Pourahmadi* and Joseph A. C. Humphrey†
University of California, Berkeley, California

Using algebraic approximations for the Reynolds stress equations a more general expression has been derived for C_μ in $\nu_t = C_\mu k^2/\epsilon$ which accounts simultaneously for the effects of streamline curvature and pressure strain in the flow, with the latter including wall-dampening effects. The new expression encompasses the less general formulations proposed earlier in the literature. It has been used in conjunction with a k-ϵ model of turbulence to predict developing, two-dimensional, curved channel flows. In general, predictions are in good agreement with experimental measurements of mildly and strongly curved flows. The model tends to overpredict the kinetic energy of turbulence in the inner-radius (convex) wall region of strongly curved flows. This failing is attributed to a breakdown of the assumption that $\overline{u_i u_j}/k$ is a constant in the model. Notwithstanding this limitation, the present formulation provides a degree of generality not previously available in two-equation modeling of confined turbulent flows with curvature.

Nomenclature

C_w = constant in Eq. (20)
C_μ = modified coefficient in Eq. (1) (includes curvature and pressure-strain effects)
$C_{\mu 0}$ = unmodified coefficient in Eq. (2)
D = channel width
D_{ij} = Reynolds stress diffusive transport term
f = wall-dampening function, $\equiv f(\ell/y)$
G_T = Görtler parameter, $\equiv 43(\theta/R_0)^{1/2}$
k = kinetic energy of turbulence
ℓ = modified length scale of turbulence (includes curvature and pressure-strain effects)
ℓ_0 = unmodified length scale of turbulence
m = experimental coefficient in Eq. (21)
P = mean pressure; also, production of k in Appendix
P_{ij} = Reynolds stress production term
R_c = channel mean radius of curvature, $\equiv (r_i + r_0)/2$
Re = Reynolds number, $\equiv DU_m/\nu$
R_o = concave wall radius of curvature (corresponds to r_o in a curved channel)
r = radial coordinate
r_i = inner-radius (convex) wall
r_o = outer-radius (concave) wall
U_m = maximum (streamwise) velocity
U_r = radial component of mean velocity
U_θ = streamwise component of mean velocity
$\overline{u_i u_j}$ = components of Reynolds stress tensor
$\overline{u_i u_j u_k}$ = triple velocity correlation
v_0 = unmodified velocity scale of turbulence
y = distance along normal to a curved wall (into the flow)
β = empirical constant in Eq. (3)
δ = extra strain in Eq. (3), $\equiv \dfrac{U_\theta}{r} \Big/ \dfrac{\partial U_\theta}{\partial r}$
δ_{ij} = Kronecker delta
ϵ = rate of dissipation of kinetic energy of turbulence
ϵ_{ij} = Reynolds stress viscous dissipation term
η = normalized radial coordinate, $\equiv (r - r_i)/(r_o - r_i)$
θ = streamwise coordinate; also, boundary-layer momentum thickness
κ = von Kármán universal constant
λ = spacing between Taylor-Görtler vortices
μ = laminar viscosity
μ_{eff} = effective viscosity, $\equiv \mu + \mu_t$
μ_t = turbulent viscosity
ν = laminar kinematic viscosity
ν_t = turbulent kinematic viscosity, $\equiv \mu_t/\rho$
Π_{ij} = Reynolds stress pressure-strain redistribution term
ρ = density
σ_k = Prandtl number for kinetic energy of turbulence
σ_ϵ = Prandtl number for dissipation
τ_w = wall shear stress

Received Dec. 11, 1981; revision received Dec. 6, 1982.

*Research Graduate Student, Dept. of Mechanical Engineering.
†Associate Professor, Dept. of Mechanical Engineering.

Introduction

THE importance of experimental measurements and theoretical predictions of turbulent flows over convex and concave surfaces and in curved channels is evidenced by the attention which these two topics have and continue to receive in relation to, for example, flow cooling and erosion of turbine blades and rocket nozzles, flows in compressors, turbomachinery, curved diffusers, and channel passages. Cases of studies pertaining to flows over convex surfaces are given in Refs. 1-8 while similar examples pertaining to flows over concave surfaces are available in Refs. 4-8. Curved channel studies have been reported in Refs. 9-19.

In an extensive review of the subject Bradshaw[20] discusses the sensitivity of turbulent flow characteristics to even small amounts of mean streamline curvature. Thus, for example, in the early study by Kreith[21] and in subsequent investigations by Thomann[22] and Mayle et al.[23] it has been shown that the heat flux through the concave wall of a curved channel can be up to 33% larger, and through the convex wall 15% smaller, relative to that through the walls of a straight channel. A similar experimental heat transfer study by Brinich and Graham[14] (not entirely free of side wall-driven secondary motion) confirms this result and, in addition, shows that while friction on the inner curved wall of a channel can fall below the values for a straight channel, friction measurements on the outer curved wall yield increases of about 50%.

Three-Dimensional Motions and the Prediction of Curved Channel Flows

Detailed measurements of the longitudinal velocity component in a turbulent curved channel flow, obtained by Hunt and Joubert,[15] have revealed Taylor-Görtler vortices[24-26] in the flow. Similar structures have arisen in other curved

channel flows, both in laminar[4,18,27] and turbulent regime,[4,9,10,19] and in boundary layers developing on concave walls.[4,12,26,28] The onset and subsequent amplification of longitudinal vortices is characterized by the Görtler parameter G_T. Tani[4] shows that for $G_T \lesssim 0.35$ longitudinal vortices will be dampened in turbulent flow, while for values $G_T \gtrsim 0.35$ amplification depends on the value of the vortex spacing parameter $\lambda\theta$ and the curvature parameter λR_c.

Ellis and Joubert[10] specifically remark on having observed Taylor-Görtler vortices for a radius ratio $R_c/D=30$ but not for $R_c/D=6$. Similarly, Crane and Winoto[19] observed a collapse of these organized structures for $Re \gtrsim 16{,}000$. While these findings contradict expectations based on stability considerations, they suggest that turbulent diffusion and pressure redistribution may be responsible for smearing out three-dimensional time-averaged structures which otherwise would be observed near the concave wall of a strongly curved channel. This suggests that the net effect of these structures can be looked upon as contributing to the overall process of turbulent mixing in the concave wall region of the flow.

Although concavely curved turbulent flows are prone to three-dimensional instabilities, for purposes of numerical computation they are commonly presumed to be two-dimensional in their mean structure. In Ref. 7, boundary-layer and curved channel predictions of longitudinal velocity showed good agreement with experimental measurements based on this assumption. However, similar calculations for friction factors[6] and turbulent shear stress[12] seriously underpredict the values of these parameters in the concave wall flow region. Likewise, while fully developed curved channel longitudinal velocity predictions of Ref. 7 are in good agreement with experimental measurements of Ref. 10 for $R_c/D=6$ over most of the channel width, near the concave wall the velocity is underpredicted by approximately 9%. While one might attribute the above discrepancies to three-dimensional Taylor-Görtler vortices as suggested in Ref. 12, within the context of a two-dimensional calculation it seems reasonable to suggest that the influence of streamline curvature and/or wall effects on turbulent mixing were underestimated at the concave walls of the above flows. In fact, higher levels of turbulent diffusion existed than were actually predicted by the models employed.

The Present Contribution

In principle, turbulence closure methods based on the calculation of modeled Reynolds stress transport equations can rigorously account for streamline curvature, pressure-strain, and wall pressure fluctuations in curved channel flows.[2,6] Simpler approaches based on a two-equation (k-ϵ) model of turbulence appear to require an empirical modeling of curvature effects in the equation for dissipation of kinetic energy of turbulence and the corresponding definition of an additional model constant which must be optimized numerically.[7] Even simpler approaches based on the mixing length concept are seriously limited by the need to prescribe different mixing-length variations for differently curved flows.[11]

The present work shows how the k-ϵ model of turbulence can be rigorously extended to predict developing curved channel flows by making C_μ in the expression for turbulent viscosity

$$\mu_t/\rho = C_\mu \underbrace{(k^{3/2}/\epsilon)}_{\ell_0} \underbrace{k^{1/2}}_{v_0} \tag{1}$$

an appropriate function of streamline curvature while simultaneously accounting for pressure-strain and wall-induced pressure fluctuation effects. In Eq. (1) the symbols ℓ_0 and v_0 denote characteristic length and velocity scales of turbulence, respectively, and are determined from transport equations for k an ϵ. The essence of the approach pursued in this study is then, that the product $C_\mu \ell_0$ in Eq. (1) should yield a modified length scale of turbulence (ℓ) which reflects the direct influence of streamline curvature and pressure strain in the flow. Calling $C_{\mu 0}$ the value of C_μ in the absence of these effects it is clear that

$$\ell = (C_\mu/C_{\mu 0})\ell_0 \tag{2}$$

If the local-equilibrium approximation is made it can be shown[29] that $C_{\mu 0} \simeq 0.12$. The recommended experimental value is $C_{\mu 0}=0.09$. It should be noticed that for models based on the notion of a turbulent viscosity as defined by Eq. (1) it is immaterial which of the two scales (ℓ_0 or v_0) is modified to include the influence of curvature (and related) effects. However, because it is consistent with subsequent modifications to be made to the turbulence model, it will be the length scale which is modified in this work. This approach is also consistent with that proposed by Bradshaw[20] on heuristic grounds for mildly curved flow, and parallels to some extent various ideas set forth in Refs. 2, 6, and 29-31.

The more general expression derived here for C_μ includes as subsets specialized expressions derived in Refs. 29-31 and yields as a special limiting case Bradshaw's proposal for the turbulent length scale in mildly curved channel flows.[20]

$$\ell = \left(1 \pm \beta \frac{U_\theta/r}{\partial U_\theta/\partial r}\right)\ell_0 \tag{3}$$

In Eq. (3), β is an empirical constant of order 10, r is the radial coordinate direction (transverse to the flow), and U_θ is the local value of the streamwise component of mean velocity along a streamline with radius of curvature r.

The extended form of the k-ϵ model presented here, with its more general formulation for C_μ, offers a compromise between the potentially more accurate but computationally more costly full Reynolds stress model closure, and the simpler but considerably more restrictive mixing-length calculation approach. In this study, attention is fixed principally on channel flows with strong curvature ($R_c/D \lesssim 20$) arising frequently in practice. However, the general formulation also applies to mildly curved channel flows and these have been predicted successfully.

Governing Equations and Boundary Conditions

Continuity and momentum equations governing steady, two-dimensional, turbulent, incompressible, developing curved channel flow in cylindrical coordinates (Fig. 1) are given by

Continuity

$$\frac{\partial U_r}{\partial r} + \frac{1}{r}\frac{\partial U_\theta}{\partial \theta} + \frac{U_r}{r} = 0 \tag{4}$$

r Momentum

$$\rho\left[U_r\frac{\partial U_r}{\partial r} + \frac{U_\theta}{r}\frac{\partial U_r}{\partial \theta} - \frac{U_\theta^2}{r}\right] = -\frac{\partial P}{\partial r} + \frac{1}{r}\frac{\partial}{\partial r}\left(\mu_{\text{eff}} r \frac{\partial U_r}{\partial r}\right) + \frac{1}{r}\frac{\partial}{\partial \theta}\left(\mu_{\text{eff}}\frac{1}{r}\frac{\partial U_r}{\partial \theta}\right) - \mu_{\text{eff}}\frac{U_r}{r^2} - \mu_{\text{eff}}\frac{2}{r^2}\frac{\partial U_\theta}{\partial \theta} + S_r \tag{5}$$

θ Momentum

$$\rho\left[U_r\frac{\partial U_\theta}{\partial r} + \frac{U_\theta}{r}\frac{\partial U_\theta}{\partial \theta} + \frac{U_r U_\theta}{r}\right] = -\frac{1}{r}\frac{\partial P}{\partial \theta} + \frac{1}{r}\frac{\partial}{\partial r}\left(\mu_{\text{eff}} r \frac{\partial U_\theta}{\partial r}\right) + \frac{1}{r}\frac{\partial}{\partial \theta}\left(\frac{\mu_{\text{eff}}}{r}\frac{\partial U_\theta}{\partial \theta}\right) - \mu_{\text{eff}}\frac{U_\theta}{r^2} + \mu_{\text{eff}}\frac{2}{r^2}\frac{\partial U_r}{\partial \theta} + S_\theta \tag{6}$$

In the above equations the Reynolds stresses have been modeled according to the Boussinesq assumption which relates the stresses to velocity gradients through a turbulent viscosity. The terms S_r and S_θ in Eqs. (5) and (6) are given by

$$S_r = \frac{1}{r}\frac{\partial}{\partial \theta}\left[\mu_t r \frac{\partial}{\partial r}\left(\frac{U_\theta}{r}\right)\right] + \frac{1}{r}\frac{\partial}{\partial r}\left(\mu_t r \frac{\partial U_r}{\partial r}\right) - \mu_t\frac{U_r}{r^2} \tag{7}$$

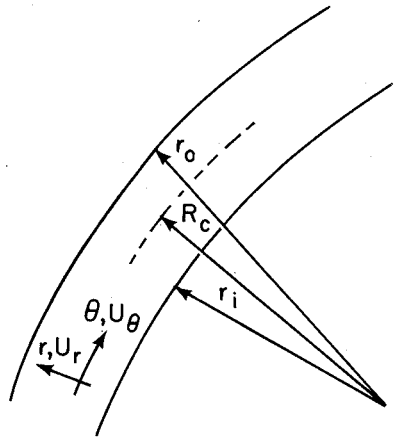

Fig. 1 Curved channel configuration and coordinate system.

Table 1 Boundary conditions for curved channel flows

	Inlet plane	Exit plane	At curved walls
U_θ	Prescribed from experiment	$\frac{\partial U_\theta}{\partial \theta}=0$ or prescribed from experiment	τ_w specified through Eq. (12)
U_r	0	$\frac{\partial U_r}{\partial \theta}=0$	0
k	$0.005(U_\theta^2)_{\text{inlet}}$	$\frac{\partial k}{\partial \theta}=0$	Prescribed from a simplification of the k and ϵ equations at the walls. See discussion in text.
ϵ	$\frac{(k^{3/2})_{\text{inlet}}}{0.01D}$	$\frac{\partial \epsilon}{\partial \theta}=0$	

$$S_\theta=\frac{1}{r}\frac{\partial}{\partial\theta}\left[\mu_t\left(2\frac{U_r}{r}+\frac{1}{r}\frac{\partial U_\theta}{\partial\theta}\right)\right]+\frac{\partial}{\partial r}\left[\frac{\mu_t}{r}\left(\frac{\partial U_r}{\partial\theta}-U_\theta\right)\right]+\frac{\mu_t}{r}\left(\frac{\partial U_\theta}{\partial r}-\frac{U_\theta}{r}\right) \tag{8}$$

In order to solve for the spatial variation of μ_t, transport equations are required for k an ϵ. Following the modeling approach outlined in Ref. 32 (based on the earlier work of Refs. 33 an 34 but restricted here to two-dimensional cylindrical coordinates) yields

Kinetic energy of turbulence, k

$$\rho\left[U_r\frac{\partial k}{\partial r}+\frac{U_\theta}{r}\frac{\partial k}{\partial\theta}\right]=\frac{1}{r}\frac{\partial}{\partial r}\left(\frac{\mu_{\text{eff}}}{\sigma_k}r\frac{\partial k}{\partial r}\right)+\frac{1}{r^2}\frac{\partial}{\partial\theta}\left(\frac{\mu_{\text{eff}}}{\sigma_k}\frac{\partial k}{\partial\theta}\right)+G-\rho\epsilon \tag{9}$$

Dissipation of kinetic energy of turbulence, ϵ

$$\rho\left[U_r\frac{\partial \epsilon}{\partial r}+\frac{U_\theta}{r}\frac{\partial \epsilon}{\partial\theta}\right]=\frac{1}{r}\frac{\partial}{\partial r}\left(\frac{\mu_{\text{eff}}}{\sigma_\epsilon}r\frac{\partial \epsilon}{\partial r}\right)+\frac{1}{r^2}\frac{\partial}{\partial\theta}\left(\frac{\mu_{\text{eff}}}{\sigma_\epsilon}\frac{\partial \epsilon}{\partial\theta}\right)+C_{\epsilon 1}\frac{\epsilon}{k}G-C_{\epsilon 2}\rho\frac{\epsilon^2}{k} \tag{10}$$

with the production term G given by

$$G=\mu_t\left\{2\left[\left(\frac{\partial U_r}{\partial r}\right)^2+\left(\frac{1}{r}\frac{\partial U_\theta}{\partial\theta}\right)^2-\frac{U_\theta}{r}\left(\frac{1}{r}\frac{\partial U_r}{\partial\theta}+\frac{\partial U_\theta}{\partial r}\right)+\frac{U_r}{r}\left(\frac{U_r}{r}+\frac{2}{r}\frac{\partial U_\theta}{\partial\theta}\right)+\frac{1}{r}\frac{\partial U_r}{\partial\theta}\frac{\partial U_\theta}{\partial r}\right]+\left(\frac{U_\theta}{r}\right)^2+\left(\frac{\partial U_\theta}{\partial r}\right)^2+\left(\frac{1}{r}\frac{\partial U_r}{\partial\theta}\right)^2\right\} \tag{11}$$

Values of the constants in the above equations were set in accordance with the recommendations of Ref. 34: $C_{\epsilon 1}=1.44$, $C_{\epsilon 2}=1.92$, and $\sigma_k=1.0$. However, at a given radial location the value of σ_ϵ (customarily fixed to 1.3 throughout the flow) was linearly interpolated from the values arising at the convex and concave walls, respectively, as discussed by Humphrey and Pourahmadi.[35]

In order to solve Eqs. (4-6), (9), and (10), the boundary conditions summarized in Table 1 were used. The region between a curved wall and the node P closest to that wall was bridged by specifying the wall shear stress (τ_w) from the standard logarithmic velocity profile. Assuming local equilibrium of the flow in near-wall regions, the law of the wall region yields

$$\tau_w\simeq\tau_P=\frac{\rho C_{\mu 0}^{1/4}k_P^{1/2}[U_\theta]_P}{A\ell n[y_P C_{\mu 0}^{1/4}k_P^{1/2}/\nu]+B} \tag{12}$$

where subscript P denotes the grid node position nearest to the wall, y is the distance from the wall, and τ_w is the wall shear stress. Values of the law of the wall constants were set to $A=2.39$ and $B=5.45$. An attempt to include curvature effects in the law of the wall using an equivalent form of Eq. (8) in the paper by Meroney and Bradshaw[12] did not yield a significant improvement in the calculations. The simpler logarithmic relation given by Eq. (12) was adhered to.

The near-wall value of kinetic energy of turbulence, k_P, was found from its standard transport equation with the flux from the wall set equal to zero and the production term modified to include the wall shear stress as given by Eq. (12). The near-wall value of dissipation of kinetic energy, ϵ_P, was initially determined by requiring that the turbulence length scale vary linearly with distance from the wall. Substituting $(\partial U_\theta/\partial y)_P$ from the law of the wall into the simplified (near-wall region) turbulent kinetic energy balance yields

$$\epsilon_P=C_{\mu 0}^{3/4}k_P^{3/2}/\ell_0 \tag{13}$$

where the turbulence length scale is given by $\ell_0=\kappa y_P$. Following Bradshaw,[20] the influence of extra-strain curvature effects on the magnitude of the turbulence length scale near curved walls can be modeled according to Eq. (3) for regions of the flow in which $\delta\equiv|(U_\theta/r)/(\partial U_\theta/\partial r)|\lesssim 0.05$. An expression for dissipation at the near-wall node P which includes the influence of streamline curvature effects is

$$\epsilon_P=C_{\mu 0}^{3/4}k_P^{3/2}/\kappa y_P(1\pm\beta\delta_P) \tag{14}$$

General Expression for C_μ

A simple example illustrates the advantages of an improved modeling of the C_μ coefficient. Combination of Eqs. (1-3) yields the expression

$$\mu_t/\rho=C_{\mu 0}\ell_0(1\pm\beta\delta)v_0 \tag{15}$$

This equation is a limiting form of the more general relation sought in this study. While Eq. (15) accounts for the influence of mild curvature effects on the turbulence length scale ℓ_0 through the curvature parameter $(1\pm\beta\delta)$, a more general relationship is desirable in which arbitrary streamline curvature, pressure-strain, and wall-dampening effects are *simultaneously* included. The purpose of this section is to outline the derivation of this more general coefficient along the lines of earlier work by Rodi.[29] To some extent, the result of this analysis is implicit in the work of Gibson.[2] However, it

is important to note that in Ref. 2 attention was restricted to weakly curved flows governed by boundary-layer equations and a determination of the general form of C_μ given here would not have been possible.

The Reynolds Stress Equations

The starting point for the present analysis is the high Reynolds number form of the u_iu_j transport equation given in Ref. 36. In three-dimensional Cartesian coordinate notation‡ and neglecting molecular diffusion this equation is

$$U_k\frac{\partial\overline{u_iu_j}}{\partial x_k}=-\underbrace{\left\{\overline{u_ju_k}\frac{\partial U_i}{\partial x_k}+\overline{u_iu_k}\frac{\partial U_j}{\partial x_k}\right\}}_{P_{ij}}-\underbrace{2\nu\overline{\frac{\partial u_i}{\partial x_k}\frac{\partial u_j}{\partial x_k}}}_{\epsilon_{ij}}$$
$$+\underbrace{\overline{\frac{p}{\rho}\left(\frac{\partial u_i}{\partial x_j}+\frac{\partial u_j}{\partial x_i}\right)}}_{\Pi_{ij}}-\underbrace{\frac{\partial}{\partial x_k}\left\{\overline{u_iu_ju_k}+\overline{\frac{p}{\rho}(\delta_{jk}u_i+\delta_{ik}u_j)}\right\}}_{D_{ij}} \quad (16)$$

In the above equation P_{ij} represents the production of $\overline{u_iu_j}$ and requires no approximation. Viscous dissipation (ϵ_{ij}) and contributions to the pressure-strain term (Π_{ij}) were modeled as in Ref. 36. The forms of these terms are

$$\epsilon_{ij}=\frac{2}{3}\epsilon\delta_{ij}(\text{isotropic dissipation}) \quad (17)$$

and

$$\Pi_{ij}=\Pi_{ij,1}+\Pi_{ij,2}+\Pi'_{ij,1}+\Pi'_{ij,2} \quad (18)$$

In Eq. (18), $\Pi_{ij,1}$ represents contributions to the pressure strain arising from fluctuating velocities only, while $\Pi_{ij,2}$ accounts for the interaction between the mean strain and fluctuating velocities. The additional contributions $\Pi'_{ij,1}$ and $\Pi'_{ij,2}$ represent pressure-strain corrections due to the effect of walls on the level of turbulent fluctuations in the flow. The terms in Eq. (18) were approximated according to model 2 of Ref. 36. A tabulated summary of the model and of the necessary model constants is given in Ref. 35.

The diffusive transport of $\overline{u_iu_j}$ is attributed primarily to turbulent velocity fluctuations for which the simple gradient diffusion hypothesis of Daly and Harlow[37] yields

$$-\overline{u_iu_ju_\ell}=C'_s\frac{k}{\epsilon}\overline{u_\ell u_m}\frac{\partial\overline{u_iu_j}}{\partial x_m} \quad (19)$$

where C'_s is an empirically determined constant (not needed in this study).

The f Wall Function

In the approximations for $\Pi'_{ij,1}$ and $\Pi'_{ij,2}$ a wall function, $f(\ell/y)$, must be specified whose role it is to diminish the magnitude of the wall pressure correction to the total pressure strain with increased distance from the wall (y). The form of the f function depends on the length scale ℓ of the energy-containing eddies and for straight channel flows is given by[36]

$$f\left(\frac{\ell}{y}\right)\equiv f=\frac{k^{3/2}}{C_w\epsilon}\left[\frac{1}{y}+\frac{1}{D-y}\right] \quad (20)$$

where D is the channel width. Equation (20) reflects the fact that distance-weighted contributions to f at any point in the flow arise from both walls. In the expression, the constant C_w is chosen such that $f\to 1$ as $y\to 0$. Thus, setting $\epsilon=C_{\mu 0}^{3/4}k^{3/2}/\kappa y$ (the inertial sublayer value) in Eq. (20) yields $C_w=\kappa/C_{\mu 0}^{3/4}$.

‡The model equations were formulated and used in cylindrical coordinates. Cartesian notation is used here for convenience.

For straight channel flows the function f is symmetrical with respect to the symmetry plane, where it possesses a minimum value. This is consistent with the notion that at the symmetry plane the walls of a straight channel should generate equivalent pressure corrections to the pressure-strain terms. The same will not be the case for channel flows in which an asymmetric condition exists; for example, straight channel flows with one smooth wall and one rough wall, and curved channels flows. In these cases the position of the minimum value of f in the flow will be shifted toward the wall contributing least to changes in the turbulence by wall pressure-fluctuation effects (i.e., the convex wall in a curved channel or the smooth wall in an asymmetrically roughened channel). In this work the location for the minimum in the f function has been assumed to coincide with the location of zero turbulent shear stress. This is consistent with the notion that the length scale of the energy-containing motion, which also transmits the pressure-fluctuation effects, should be smallest at the zero shear stress position; see, for example, the data in Ref. 9, and Eq. (30) and related discussion in Ref. 2. In this way the flow is divided into two regions in either one of which the wall nearest to that region is the major source of wall-induced contributions to the pressure-strain correlation.

A general expression for f which accommodates both the symmetric and asymmetric conditions referred to above is

$$f=\frac{k^{3/2}}{C_w\epsilon}\left[\frac{1}{y}+\frac{(y/D)^m}{D-y}\right] \quad (21)$$

In Eq. (21) y is taken as the distance into the flow measured from the wall which induces the largest contributions to the wall-correction terms; i.e., the concave wall in a curved channel. The value of m can be determined from available experimental data as described in Ref. 35, where it is found that $m=7.95$ for $R_c/D\lesssim 20$ and $m=2.56$ for $R_c/D>20$. For $m=0$ Eq. (21) reduces to the straight channel result given by Eq. (20).

Derivation of the C_μ Function

Following Rodi,[29] algebraic expressions for the Reynolds stresses are obtained from Eq. (16) by assuming that along a streamline the net transport of u_iu_j is proportional to the net transport of k multiplied by the factor u_iu_j/k. The same assumption was made by Gibson[2] in his curved flow study. Although inexact, for example see discussion by Ramaprian and Shivaprasad,[8] the assumption is a reasonable one for thin shear layer flows and has been used successfully by, among others, Ljuboja and Rodi[30] for wall jets, El Tahry et al.[38] for passive scalar dispersal, and by Gibson and Launder[39] in free shear flows under gravitational influence. With this assumption, Eq. (16) simplifies to[35]

$$\frac{\overline{u_iu_j}}{k}[G-\epsilon]=P_{ij}-\epsilon_{ij}+\Pi_{ij} \quad (22)$$

from which algebraic relations for the Reynolds stresses are obtained. The general form of C_μ is derived by equating the algebraic expression for $\overline{u_\theta u_r}$ with the Boussinesq approximation for $u_\theta u_r$ in which μ_t is given by Eq. (1). Because the derivation in cylindrical coordinates is lengthy, the reader is referred to Humphrey and Pourahmadi[35] for details. The final result is

$$C_\mu^{1/2}=2Q^{1/2}\cos\left[\frac{1}{3}\cos^{-1}(RQ^{-3/2})\right]-\frac{S}{3} \quad (23)$$

where Q, R, and S are complex algebraic expressions (given in the Appendix) depending on velocity gradients, the wall function f, the ratio G/ϵ, and the turbulence model constants. It is important to note that in deriving Eq. (3) boundary-layer approximations are not made and the result applies to fully elliptic flows.

Limiting Expressions for the C_μ Function

The general expression for C_μ given by Eq. (23) has several interesting limiting forms attesting to its validity. These have been obtained in Ref. 35 and correspond to the following cases: 1) variation of C_μ for flow in the presence of a flat wall[30]; 2) variation of C_μ for flow with variable G/ϵ[29]; 3) variation of C_μ for flow with streamline curvature[31]; and 4) variation of C_μ for flow with small δ in the presence of a curved wall.

In particular, case 4 yields

$$C_\mu = 0.056[1 - 12.17\delta + 0(\delta^2)] \tag{24}$$

Comparing Eq. (24) with Eq. (2), and recalling Eq. (3), shows that $C_{\mu 0} = 0.056$ and $\beta = 12.17$. This value for β is in good agreement with the values recommended in the literature. For example, Eide and Johnston[40] suggest $\beta = 12$ for both concave and convex walls, while Bradshaw[20] recommends $\beta = 9$ at a concave wall and $\beta = 14$ at a convex wall. Similarly, the value for $C_{\mu 0}$ obtained here falls in the range of values calculated for turbulent wall jets in Ref. 30 where the authors find $C_\mu \simeq 0.05$ in the near wall region of their jet flow.

The Numerical Scheme

It is required to solve the transport equations [Eqs. (4), (6), (9), and (10)] in conjunction with the boundary conditions summarized in Table 1. Finite difference equations are obtained by volume integration of the transport equations over control volumes or "cells" into which the flow domain is discretized. Details concerning the method for deriving the difference equations and the inclusion of boundary conditions are provided in, for example, Refs. 41 and 42, while an exposition and thorough discussion of the philosophy underlying the calculation approach is available in Ref. 43.

The numerical procedure used to solve the finite difference equations was the Imperial College "TEACH-2E" code.[44] Together with appropriately differenced boundary conditions, elliptic forms of the equations are solved by means of the SIMPLE algorithm.[43] For each iteration, various sweeps are made of the entire calculation domain along the main flow direction until a pre-established convergence criterion is satisfied. The choice of a numerical procedure solving elliptic equations was dictated by the desire to compute flows where, even though streamwise recirculation may be absent, ellipticity in the pressure field can significantly affect the flow.[45]

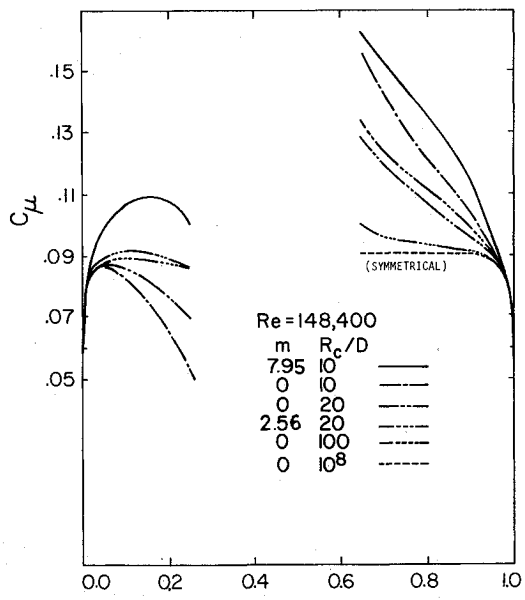

Fig. 2 Transverse variation of C_μ in fully developed curved and straight channel flow. For $m = 0$ wall function f is symmetric. Calculations based on extended k-ϵ model.

Calculated Results and Discussion

This section summarizes the main results obtained in applying the extended turbulence model with the general expression for C_μ to mildly and strongly curved channel flow configurations. A more detailed presentation of these and related findings is available in Ref. 35.

First the assumption that $u_\theta u_r/k$ is constant along flow streamlines was considered. While it is difficult to quantify this point precisely, there is evidence in the literature that the assumption is inexact. See, for example, the measurements in Ref. 8 for mildly curved non-interacting convex and concave surfaces. Data plotted in Ref. 35 for developed curved[9,15] and straight[46] channel flows suggest that the approximation is reasonable for values of $\eta \lesssim 0.20$ and $\eta \gtrsim 0.60$ in curved channels. The assumption is invalid for $0.20 \lesssim \eta \lesssim 0.60$ and curtails the usefulness of the general expression for C_μ in this region. Figure 2 shows the variation of C_μ as a function of radial position in channels of different curvature. In general, C_μ is seen to increase at both walls of a curved channel, at a rate inversely proportional to channel curvature (defined earlier as R_c/D). At the convex wall C_μ reaches a maximum value at a radial location dictated by the channel curvature. As of this location C_μ diminishes with increased distance from the inner-radius wall. For strong curvatures the general function for C_μ yielded unrealistic values of this parameter in the region $0.30 \lesssim \eta \lesssim 0.65$ due to the lack of constancy in the ratio $u_i u_j/k$. However, calculations revealed an insensitivity of the numerical results toward the value of C_μ in this flow region provided that it was contained within the range $0.045 \lesssim C_\mu \lesssim 0.140$. This insensitivity is explained, in part, by the small values of $\partial U_\theta/\partial r$ and the respectively counteracting curvature influences which arise in the core region of curved channel flow. In the present study C_μ was fixed to the recommended value of 0.09 in the region $0.30 \lesssim \eta \lesssim 0.65$.

Wall curvature and wall pressure fluctuations contribute jointly to the value of C_μ. In an effort to separate these two effects, and thereby establish their relative importance, two sets of C_μ profiles in Fig. 2 ($R_c/D = 10$ and 20) have been calculated with a symmetric distribution of the f function imposed ($m = 0$); equivalent to specifying a straight channel flow condition insofar as wall pressure corrections are concerned, while retaining the direct influences of the respective wall curvatures on C_μ. Inspection of these profiles shows that curvature at the concave wall acts to enhance C_μ while curvature at the convex wall acts to suppress it. The inclusion of wall pressure corrections in the pressure strain ($m = 2.56$, $m = 7.95$) further increases C_μ at both walls, but at the convex wall the direct influence of curvature effects ultimately overcomes the wall pressure contribution to C_μ causing a net decrease in its value with increasing distance from the convex wall.

Plots of the f function, given in Ref. 35 for various curvature ratios, show decreasing values of f with increased distance from either channel wall, reflecting the decreased influence of wall corrections on the turbulent flow. These plots also show that at a fixed radial location the f wall function decreases strongly with increased curvature at the convex wall, while it increases only slightly in the concave wall region bounded by $0.85 \lesssim \eta \lesssim 1$. These observations are in agreement with the algebraic stress model predictions in Ref. 2 and illustrate the point that convex surfaces are considerably less effective in redistributing wall-pressure contributions in turbulent flows than are concave surfaces. Since C_μ can be shown to be inversely proportional to the f wall function, the above observations suggest that pressure fluctuations will contribute more strongly to C_μ at the convex wall than at the concave wall with increasing channel curvature. That this is the case is confirmed by comparing the relative increase between pairs of inner-radius wall C_μ profiles in Fig. 2 (with the different f functions specified) for $R_c/D = 20$ and 10. By contrast, relative changes in the C_μ profiles at the outer-radius wall are smaller and of comparable magnitude for both

curvatures. This suggests that it is principally the direct influence of curvature effects which determines the shape of the C_μ profiles in the outer-radius or concave flow region, with the magnitude of C_μ being changed only slightly by the wall-pressure correction term. It should be noticed that the same η cut-off values fixed for C_μ apply to the f wall function since in the present model the influence of the latter parameter appears exclusively through the former.

Prior to conducting curved channel flow predictions, the calculation scheme and the present turbulence model were tested by reference to the straight channel turbulent flow measurements of Laufer.[46] This test case has also been calculated by Hanjalic and Launder[47,48] using a full Reynolds stress turbulence model. Predictions here were made with a standard k-ϵ model ($C_\mu = 0.09$; $f = 0$) and with the extended k-ϵ model containing the general C_μ expression. While all three models showed excellent agreement between calculated and measured velocity profiles, it was found that the inclusion of wall pressure corrections in the present formulation for C_μ led to a considerably improved prediction of turbulent kinetic energy throughout the whole channel.

Typical predictions of flow velocity, friction factor, and kinetic energy of turbulence are presented in Figs. 3-7 for mildly and strongly curved channel flows. Calculations of mean velocity corresponding to the mildly curved ($R_c/D = 100$) channel geometry of Hunt and Joubert[15] provided in Fig. 3 show very good agreement with the measurements. Minor differences are displayed between measurements and calculations at $R_c\theta/D = 36$ and 60 in the inner- and outer-radius wall regions. These are attributed to the presence of weak Taylor-Görtler type secondary motions which were observed in the measurements. Mean velocity calculations for the strongly curved channel configuration of Eskinazi and Yeh[9] ($R_c/D = 9.5$) are plotted in Fig. 4. For this case the discrepancies are larger between measurements and calculations near the outer-radius wall. However, differences are reduced slightly when the more general expression for C_μ given by Eq. (23) is employed. As before, the discrepancies are attributed to the presence of Taylor-Görtler vortices, evidenced in the shear stress measurements of this flow.[9]

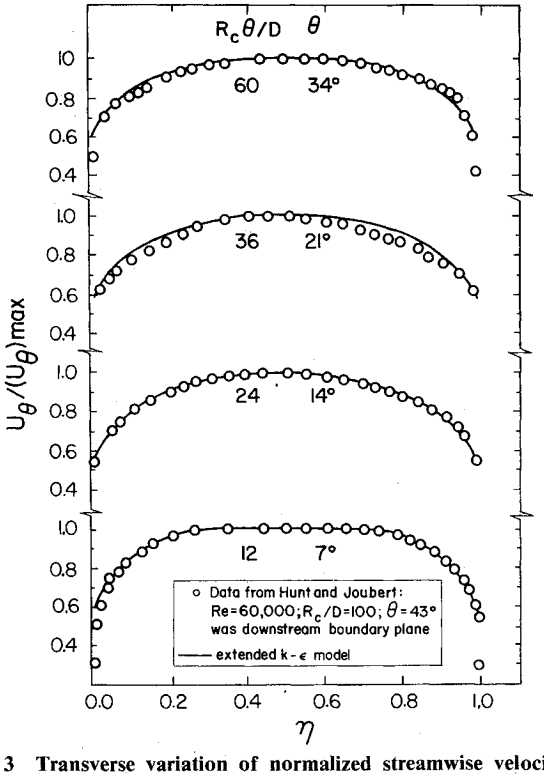

Fig. 3 Transverse variation of normalized streamwise velocity in developing mildly curved channel flow.

Measurements of the friction coefficient from the study of Honami et al.[11] are compared in Fig. 5 with calculations conducted at three levels of turbulence model refinement. The best results correspond to the extended k-ϵ model with the general C_μ formulation, and in which length-scale curvature adjustments are incorporated in the calculation of dissipation and dissipation Prandtl number near the walls. While the agreement between measurements and calculations with the extended model is very good at the inner-radius wall, it is at the outer wall where inclusion of the above effects produces the largest improvements. Calculations of the friction coefficient for the flow of Eskinazi and Yeh also yielded similar levels of improved agreement when using the extended version of the k-ϵ model offered here.

Calculations of the kinetic energy of turbulence for the channel flow of Eskinazi and Yeh are presented in Fig. 6. The profiles showing the best overall agreement with the measurements correspond to the extended model, although differences between models are seen to decrease toward the center of the flow. Calculations in the outer-radius wall region are in better agreement with the measurements than at the inner wall. When contrasted with similar predictions[35] of kinetic energy of turbulence for the mildly curved flow of Hunt and Joubert, the results suggest that the magnitude of the discrepancy in the inner-radius wall region is inversely proportional to the curvature ratio (R_c/D); for the strongly curved flow of Eskinazi and Yeh the level of k is overpredicted by between 30 to 50% while for the flow of Hunt and Joubert an overprediction of less than 20% is observed.

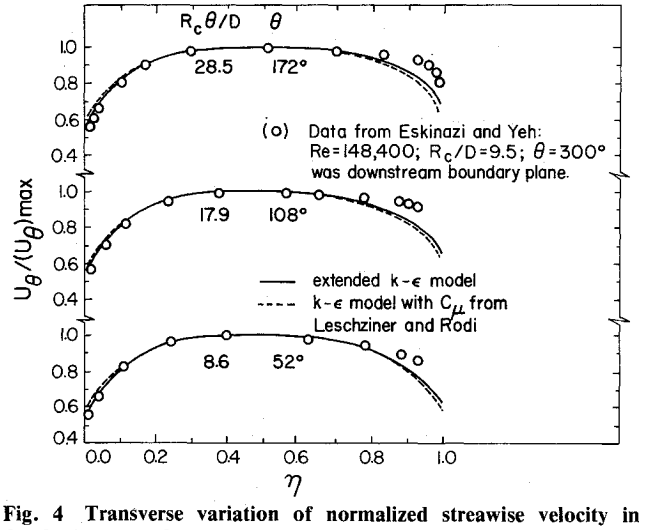

Fig. 4 Transverse variation of normalized streawise velocity in developing strongly curved channel flow.

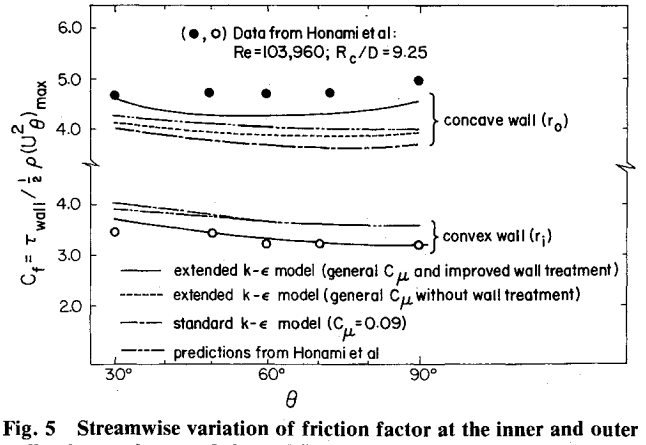

Fig. 5 Streamwise variation of friction factor at the inner and outer walls of strongly curved channel flow.

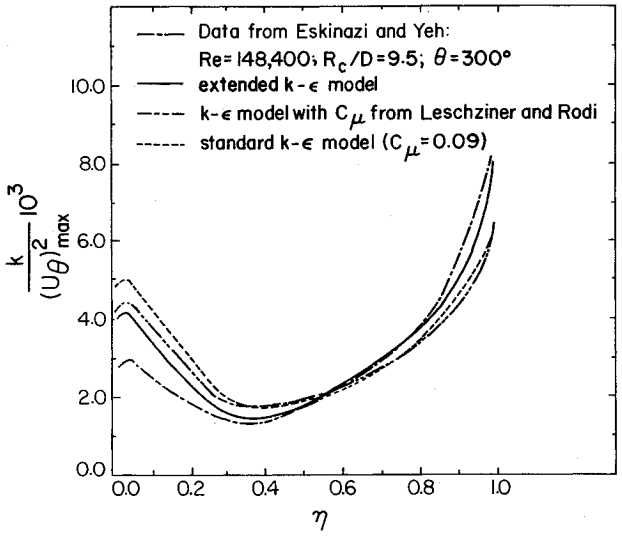

Fig. 6 Transverse variation of normalized kinetic energy of turbulence in strongly curved channel flow.

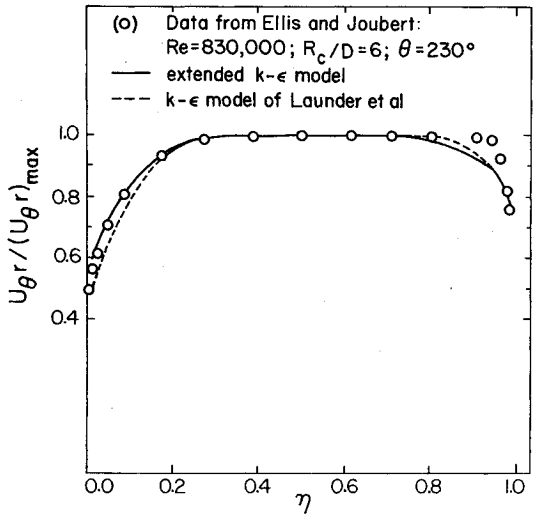

Fig. 7 Transverse variation of normalized angular momentum in strongly curved channel flow.

Calculations corresponding to the mean velocity measurements of Ellis and Joubert[10] are shown in Fig. 7 where they are compared with calculations by Launder et al.[7] using a k-ϵ model of turbulence developed along the lines of Jones and Launder.[49] In the model of Launder et al.[7] curvature effects on the length scale of the flow are included via an empirical modification to the dissipation equation. This consists of making the coefficient $C_{\epsilon 2}$ in Eq. (10) a function of a turbulent Richardson number. The approach has been criticized by both Gibson[2] and by Rodi,[50] who argue that the appropriate place to make such a modification is in the production term of the dissipation equation. Effectively, it is the latter approach which has been developed in this study. The predictions of Launder et al.[7] show slightly better agreement with the measurements at the outer-radius wall, but over a large portion of the inner-wall region the present model yields better results. It is difficult to decide on the basis of this comparison which model is more accurate for the prediction of curved channel flows in general. However, in view of the points raised by Gibson[2] and Rodi,[50] and given the fact that the model of Launder et al.[7] requires an additional, (numerically optimized) constant, it would seem that the model offered here is of a more general nature.

Conclusions

Using Reynolds stress equations in algebraically modeled form a general expression has been derived for the coefficient C_μ in the expression for turbulent viscosity $\mu_t/\rho=C_\mu k^2/\epsilon$. The generalized form of this coefficient includes streamline curvature and pressure-strain effects (including wall corrections) *simultaneously* and, hence, their respective influence on the turbulent length scale ($k^{3/2}/\epsilon$) in the flow. The expression derived has been shown to reduce to limiting forms of less general formulations obtained in other works.[35] One of these forms corresponds to the proposal by Bradshaw, Eq. (3), and yields values of the constants $\beta=12.17$ and $C_{\mu 0}=0.056$ which are in agreement with values established in the literature.

Predictions of developing, two-dimensional, curved channel flow have been conducted by incorporating the general expression for C_μ into a k-ϵ model of turbulence. The model has also been modified to include the direct influence of curvature effects on the length scale in near-wall regions of the flow. In general, agreement between measurements and calculations of mean velocity, shear stress, and kinetic energy of turbulence are good. The discrepancies observed in the calculations of mean velocity arise at the outer-radius or concave wall and are attributed to the existence of cross-stream motions (Taylor-Görtler vortices) in the experiments. The present turbulence model consistently overpredicts the kinetic energy of turbulence in the inner-radius or convex wall region of curved channel flow. The degree of overprediction (less than 35% for the worst case) appears to be inversely proportional to mean channel curvature (R_c/D). The overprediction is attributed to a failing in the model to accommodate fully the stabilizing influences of convex curvature on turbulent flow. It is believed that this failing is related to a breakdown of the assumption that $u_i u_j/k$ is constant along flow streamlines.

It is a noteworthy feature of the extended k-ϵ model presented here that no previously established model constants have been modified to improve agreement between predictions and measurements. The new parameter m appearing in the f wall function was determined from experimental measurement as opposed to numerical optimization. In this sense, the present turbulence model provides a more general formulation than models based on the ad-hoc inclusion of a flux Richardson number in the equation for dissipation of turbulent kinetic energy.

Appendix

Expressions for Q, R, and S, for calculating C_μ from Eq. (23) are provided here. Their detailed derivation is given in Ref. 35.

$$Q=(3a_2-a_1^2)/9$$

$$R=(9a_1a_2-27a_3-2a_1^3)/54$$

$$S=[R+(Q^3+R^2)^{1/2}]^{1/3}$$

In these expressions a_1, a_2, and a_3 are given by the algebraic relations listed below. It is important to note that the first sign for a_1 and a_3 should be taken when $\partial U_\theta/\partial r>0$, and the second sign when $\partial U_\theta/\partial r<0$.

$$a_1=\pm\frac{2[(D+P/\epsilon)(1-B)-F(A-1+P/\epsilon)]\delta_b(P/\epsilon)^{1/2}}{(D+P/\epsilon)(A-1+P/\epsilon)[(1-\delta+\delta_c)^2+4\delta_b^2]^{1/2}}$$

$$a_2=\{-E(2\delta-\delta_c)\{(A-1+P/\epsilon)[2F(1+\delta)$$

$$+2C_2C_2'f(2\delta-\delta_c)]+2C_1'f(1-B)(\delta_c-2\delta)\}$$

$$+2E(D+P/\epsilon)(1-B)(\delta_c-2\delta)(1+\delta)$$

$$+4F(1-C_2)\delta_b^2(1-B)(G-1+P/\epsilon)\}P/\epsilon\div\{[(1-\delta+\delta_c)^2$$

(cont.)

$$+4\delta_b^2]\,[-(D+P/\epsilon)(A-1+P/\epsilon)(G-1+P/\epsilon)]\}$$

$$+\{-E(2\delta-\delta_c)\{\tfrac{2}{3}(D+1+P/\epsilon)(A-1+P/\epsilon)$$

$$+\tfrac{2}{3}(D+BP/\epsilon)C_1'f\}+E(1+\delta)[\tfrac{2}{3}(D+BP/\epsilon)](D+P/\epsilon)\}$$

$$\div\{-(D+P/\epsilon)(A-1+P/\epsilon)(G-1+P/\epsilon)(1-\delta+\delta_c)\}$$

$$a_3=\mp\{E(2\delta-\delta_c)\delta_b\{2(1-B)[2F(1+\delta)$$

$$+2C_2C_2'f(2\delta-\delta_c)]+4(1-B)(\delta_c-2\delta)C_2C_2'f\}$$

$$+4EF(1-B)(\delta_c-2\delta)(1+\delta)\delta_b\}\left[\frac{P/\epsilon}{(1-\delta+\delta_c)^2+4\delta_b^2}\right]^{3/2}$$

$$\div\{-(D+P/\epsilon)(A-1+P/\epsilon)(G-1+P/\epsilon)\}$$

$$\mp\{\tfrac{2}{3}E(2\delta-\delta_c)\delta_b\{2(D+HP/\epsilon)(1-B)$$

$$+2(D+BP/\epsilon)C_2C_2'f\}+(4/3)E(1+\delta)(D+BP/\epsilon)F\delta_b\}$$

$$\times\left[\frac{P/\epsilon}{(1-\delta+\delta_c)^2+4\delta_b^2}\right]^{1/2}\div\{-(D+P/\epsilon)(A-1+P/\epsilon)$$

$$\times(G-1+P/\epsilon)(1-\delta+\delta_c)\}$$

In the above equations P and ϵ represent the production and dissipation of kinetic energy of turbulence, respectively, and f is the wall function given by Eq. (20). The remaining symbols are defined by

$$A=C_1(1+2fC_1'/C_1) \qquad F=1-C_2$$

$$B=C_2(1-2fC_2') \qquad G=C_1[1+(3/2)fC_1'/C_1]$$

$$D=C_1-1 \qquad H=C_2(1+fC_2')$$

$$E=1-C_2[1-(3/2)fC_2']$$

and

$$\delta_a=\frac{\partial U_\theta}{r\partial\theta}\Big/\frac{\partial U_\theta}{\partial r} \qquad \delta_b=\frac{\partial U_r}{\partial r}\Big/\frac{\partial U_\theta}{\partial r}$$

$$\delta_c=\frac{\partial U_r}{r\partial\theta}\Big/\frac{\partial U_\theta}{\partial r} \qquad \delta=\frac{U_\theta}{r}\Big/\frac{\partial U_\theta}{\partial r}$$

The model constants are: $C_1=2.2$, $C_1'=0.75$, $C_2=0.55$, and $C_2'=0.45$.

Acknowledgments

This study was made possible by funding received from the following agencies: Office of Naval Research, Contract N00014-80-C-0031 and Division of Material Sciences, Office of Basic Energy Sciences, U.S. Department of Energy, Contract W-7405 ENG-48. We are grateful to the anonymous reviewer for bringing Ref. 8 to our attention, and to Mrs. J. Reed for the typing of this manuscript.

References

[1] Wilcox, D. C. and Chambers, T. L., "Streamline Curvature Effects on Turbulent Boundary Layers," *AIAA Journal*, Vol. 15, April 1977, pp. 574-580.

[2] Gibson, M. M., "An Algebraic Stress and Heat-Flux Model for Turbulent Shear Flow with Streamline Curvature," *International Journal of Heat and Mass Transfer*, Vol. 21, 1978, pp. 1609-1617.

[3] Simon, T. W. and Moffat, R. J., "Heat Transfer Through Turbulent Boundary Layers—The Effects of Introduction of and Recovery From Convex Curvature," ASME Paper 79-WA/GT-10, New York, N.Y., Dec. 1979.

[4] Tani, I., "Production of Longitudinal Vortices in the Boundary Layer Along a Concave Wall," *Journal of Geophysical Research*, Vol. 67, No. 8, 1962, pp. 3075-3080.

[5] Rotta, J. C., "Effects of Streamwise Wall Curvature on Compressible Turbulent Boundary Layers," *The Physics of Fluids Supplement*, 1967, pp. S174-S180.

[6] Irwin, H.P.A.H. and Smith, P. A., "Prediction of the Effect of Streamline Curvature on Turbulence," *The Physics of Fluids*, Vol. 18, No. 6, 1975, pp. 624-630.

[7] Launder, B. E., Priddin, C. H., and Sharma, B. I., "The Calculation of Turbulent Boundary Layers on Spinning and Curved Surfaces," *Transactions of ASME, Journal of Fluids Engineering*, Vol. 99, 1977, pp. 231-239.

[8] Ramaprian, B. R. and Shivaprasad, B. G., "The Structure of Turbulent Boundary Layers Along Mildly Curved Surfaces," *Journal of Fluid Mechanics*, Vol. 85, 1978, p. 273.

[9] Eskinazi, S. and Yeh, H., "An Investigation on Fully Developed Turbulent Flows in a Curved Channel," *Journal of Aeronautical Sciences*, 1956, pp. 23-34.

[10] Ellis, L. B. and Joubert, P. N., "Turbulent Shear Flow in a Curved Duct," *Journal of Fluid Mechanics*, Vol. 62, Pt. 1, 1974, pp. 65-84.

[11] Honami, S., Ariga, I., Abe, T., and Watanabe, I., "Investigation of Turbulent Flows in Curved Channels," ASME Paper 75-FE-32, May 1975.

[12] Meroney, R. N. and Bradshaw, P., "Turbulent Boundary-Layer Growth Over a Longitudinally Curved Surface," *AIAA Journal*, Vol. 13, Nov. 1975, pp. 1446-1453.

[13] Blottner, F. G., "Entry Flow in Straight and Curved Channels with Slender Channel Approximations," *Transactions of ASME, Journal of Fluids Engineering*, Vol. 99, 1977, pp. 666-674.

[14] Brinich, P. F. and Graham, R. W., "Flow and Heat Transfer in a Curved Channel," NASA TN D-8464, 1977.

[15] Hunt, I. A. and Joubert, P. N., "Effects of Small Streamline Curvature on Turbulent Duct Flow," *Journal of Fluid Mechanics*, Vol. 91, Pt. 4, 1979, pp. 633-659.

[16] So, R. M., "A Turbulence Velocity Scale for Curved Shear Flows," *Journal of Fluid Mechanics*, Vol. 70, Pt. 1, 1975, pp. 37-57.

[17] Prabhu, A. and Sundarasiva Rao, B. N., "On the Large-Scale Structure in Turbulent Boundary Layers on Curved Surfaces," Paper presented at the Joint ASME/ASCE Mechanics Conference, University of Colorado, Boulder, Colo., June 1981.

[18] Winoto, S. H. and Crane, R. I., "Vortex Structure in Laminar Boundary Layers on a Concave Wall," *International Journal of Heat and Fluid Flow*, Vol. 2, 1980, p. 221.

[19] Crane, R. I. and Winoto, S. H., "Longitudinal Vortices in a Concave Surface Boundary Layer," *Turbulent Boundary Layers —Experiments, Theory and Modeling*, AGARD CP 271, Paper 9, 1980.

[20] Bradshaw, P., *Effects of Streamline Curvature on Turbulent Flow*, AGARDograph 169, 1973.

[21] Kreith, F., "The Influence of Curvature on Heat Transfer to Incompressible Fluids," *Transactions of ASME, Journal of Fluids Engineering*, Vol. 77, No. 11, 1955, pp. 1247-1256.

[22] Thomann, H., "Effect of Streamwise Wall Curvature Heat Transfer in a Turbulent Boundary Layer," *Journal of Fluid Mechanics*, Vol. 33, Pt. 2, 1968, pp. 283-292.

[23] Mayle, R. E., Blair, M. F., and Kopper, F. C., "Turbulent Boundary Layer Heat Transfer on Curved Surfaces," *Journal of Heat Transfer*, Vol. 101, No. 3, 1979, pp. 515-523.

[24] Taylor, G. I., "Stability of Viscous Liquid Contained Between Two Rotating Cylinders," *Philosophical Transactions of the Royal Society*, London, Vol. 223, 1923, pp. 289-343.

[25] Taylor, G. I., "Distribution of Velocity and Temperature Between Concentric Rotating Cylinders," *Proceedings of the Royal Society of London*, Ser. A, Vol. 151, 1935, pp. 494-512.

[26] Görtler, H., "Über Eine Dreidimensionale Instabilität Laminarer Grenz-Schichten an Konkaven Wänden," *Nachr. Ges. Wiss. Göttingen, Math.-phys. K1*, Vol. 2, No. 1, 1940; also available as NACA TM 1375, 1942.

[27] Kelleher, M. D., Flentil, D. L., and McKeen, R. J., "An Experimental Study of the Secondary Flow in a Curved Rectangular Channel," ASME Paper 79-FE-6, New York, N.Y., Dec. 1979.

[28] Patel, V. C., "Measurements of Secondary Flow in the Boundary Layers of a 180 Degree Channel," Aeronautical Research Council, Paper 1043, 1968.

[29] Rodi, W., "A New Algebraic Relation for Calculating the Reynolds Stresses," *ZAMM*, Vol. 56, 1976, pp. T219-T221.

[30] Ljuboja, M. and Rodi, W., "Calculation of Turbulent Wall Jets with an Algebraic Reynolds Stress Model," *Proceedings of the ASME Symposium on Turbulent Boundary Layers*, Niagra Falls, N.Y., June 1979.

[31] Leschziner, M. A. and Rodi, W., "Calculation of Annular and Twin Parallel Jets Using Various Discretization Schemes and Turbulence Model Variants," *Transactions of ASME, Journal of Fluids Engineering*, Vol 103, June 1981, pp. 352-360.

[32] Humphrey, J.A.C, Whitelaw, J. H., and Yee, G., "Turbulent Flow in a Square Duct with Strong Curvature," *Journal of Fluid Mechanics*, Vol. 103, 1981, pp. 443-463.

[33] Jones, W. P. and Launder, B. E., "The Prediction of Laminarization with a Two-Equation Model of Turbulence," *International Journal of Heat and Mass Transfer*, Vol. 15, 1972, pp. 301-314.

[34] Launder, B. E. and Spalding, D. B., "The Numerical Computation of Turbulent Flows," *Computer Methods in Applied Mechanics and Engineering*, Vol. 3, 1974, pp. 269-289.

[35] Humphrey, J.A.C. and Pourahmadi, F., "A Generalized Algebraic Relation for Predicting Developing Curved Channel Flow with a k-ϵ Model of Turbulence," University of California, LBL Rept. 12009 Rev., June 1981.

[36] Launder, B. E., Reece, G. J., and Rodi, W., "Progress in the Development of a Reynolds-Stress Turbulence Closure," *Journal of Fluid Mechanics*, Vol. 68, Pt. 3, 1975, pp. 537-566.

[37] Daly, B. J. and Harlow, F. H., "Transport Equations of Turbulence," *The Physics of Fluids*, Vol. 13, 1970, p. 2634.

[38] El Tahry, S., Gosman, A. D., and Launder, B. E., "The Two- and Three-Dimensional Dispersal of a Passive Scalar in a Turbulent Boundary Layer," *International Journal of Heat and Mass Transfer*, Vol. 24, 1981, p. 35.

[39] Gibson, M. M. and Launder, B. E., "On the Calculation of Horizontal Turbulent, Free Shear Flows under Gravitational Influence," *Transactions of ASME, Journal of Heat Transfer*, Ser. C, Vol. 98C, 1976, p. 81.

[40] Eide, S. A. and Johnston, J. P., "Prediction of the Effects of Longitudinal Wall Curvature and System Rotation on Turbulent Boundary Layers," Dept. of Mech. Eng., Stanford Univ., Stanford, Calif., Rept. PD-19, 1974.

[41] Humphrey, J.A.C., "Numerical Calculation of Developing Laminar Flow in Pipes of Arbitrary Curvature Radius," *Canadian Journal of Chemical Engineering*, Vol. 56, 1978, p. 151.

[42] Humphrey, J., Taylor, A., and Whitelaw, J. H., "Laminar Flow in a Square Duct of Strong Curvature," *Journal of Fluid Mechanics*, Vol. 83, 1977, pp. 509-527.

[43] Patankar, S. V., *Numerical Heat Transfer and Fluid Flow*, Hemisphere Publishing Corp., McGraw-Hill Book Co., N.Y., 1980.

[44] Gosman, A. D. and Pun, W. M., "Lecture Notes for Course Entitled: Calculation of Recirculating Flows," Imperial College, London University, Rept. HTS/74/2, 1974.

[45] Yee, G., Chilukuri, R., and Humphrey, J.A.C., "Developing Flow and Heat Transfer in Strongly Curved Ducts of Rectangular Cross Section," *Transactions of ASME, Journal of Heat Transfer*, Vol. 102, 1980, pp. 285-291.

[46] Laufer, J., "Investigation of Turbulent Flow in a Two-Dimensional Channel," NACA TN 2123, 1950.

[47] Hanjalic, K. and Launder, B. E., "A Reynolds Stress Model of Turbulence and its Application to Thin Shear Flows," *Journal of Fluid Mechanics*, Vol. 52, Pt. 4, 1972, pp. 609-638.

[48] Hanjalic, K., "Two-Dimensional Asymmetric Turbulent Flow in Ducts," Ph.D. Thesis, University of London, 1970.

[49] Jones, W. P. and Launder, B. E., "The Prediction of Laminarization with a 2-Equation Model of Turbulence," *International Journal of Heat and Mass Transfer*, Vol. 15, 1972, p. 301.

[50] Rodi, W., "Influence of Buoyancy and Rotation on Equations for the Turbulent Length Scale," *Proceedings of the 2nd Symposium on Turbulent Shear Flows,"* Imperial College, London University, July 1979.